

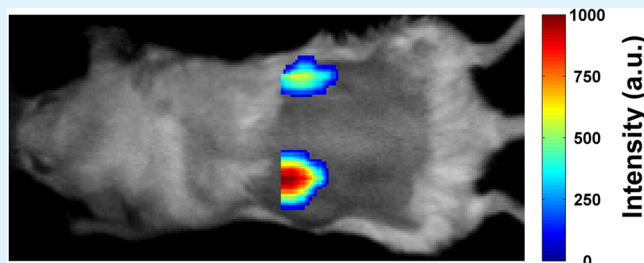
Background-Free In vivo Time Domain Optical Molecular Imaging Using Colloidal Quantum Dots

Guobin Ma*

ART Advanced Research Technologies Inc., 2300 Alfred-Nobel Boulevard, Montreal, Quebec, Canada H4S 2A4

ABSTRACT: The interest in optical molecular imaging of small animals in vivo has been steadily increased in the last two decades as it is being adopted by not only academic laboratories but also the biotechnical and pharmaceutical industries. In this Spotlight paper, the elements for in vivo optical molecular imaging are briefly reviewed, including contrast agents, i.e., various fluorescent reporters, and the most commonly used technologies to detect the reporters. The challenges particularly for in vivo fluorescence imaging are discussed and solutions to overcome the said-challenges are presented. An advanced imaging technique, in vivo fluorescence lifetime imaging, is introduced together with a few application examples. Taking advantage of the long fluorescence lifetime of quantum dots, a method to achieve background-free in vivo fluorescence small animal imaging is demonstrated.

KEYWORDS: quantum dots, fluorescence lifetime, fluorescence imaging, fluorescence lifetime imaging, in vivo small animal optical molecular imaging, time-domain molecular imaging



1. INTRODUCTION

In vivo small animal molecular imaging has gained great interest within the last two decades,^{1–8} because of its quantitative sensitivity and relative ease of use. The ultimate goal of in vivo small animal molecular imaging is to provide a tool for researchers to intactly probe the inside of a living small animal in order to obtain pathological information, monitor neurological activities, examine disease progression or regression, track drug distribution, and evaluate drug efficacy at either the cellular or the molecular level.

To reach such a goal, a contrast agent or reporter is usually required. It can be either administrated to the imaging subject or born with the animal by genetically modifying it. A device is also required to “see” the reporter. In optical imaging, the device is usually a photon detector that records the photons emitted from the reporter. Very often, the reporter needs to be activated by an external light source in order for it to emit photons. This is the case of fluorescence optical molecular imaging.⁹ Sometimes, the reporter can be activated by chemical reaction. That is the case of bioluminescence (also known as chemiluminescence or natural-luminescence) optical molecular imaging.¹⁰ It was demonstrated recently that photons are emitted when a charged particle moves faster than the speed of light in living tissue; detecting these photons to image a small animal is the so-called Cerenkov luminescence imaging.¹¹

In vivo optical molecular imaging has been widely accepted in the past decade^{2,5–8} because of its numerous advantages, for example, easy to use, low operation cost, ionizing radiation free, just to name a few. In this paper, we will focus on in vivo fluorescence optical molecular imaging. We will start by summarizing the fluorescent reporters that are frequently

used in optical molecular imaging. Then, we will review the technologies available to detect the reporters. After that, we will discuss the challenges encountered in a realistic imaging context, and introduce an imaging system aiming to overcome most of these challenges. Moreover, we will highlight the advantages of in vivo fluorescence lifetime imaging (FLIM), an advanced technique with many new potential applications, and provide some examples. We will also present a new method to obtain background-free in vivo fluorescence imaging by combining the advantages of quantum dots and time domain (TD) fluorescence molecular imaging technology. We will end this paper with a summary and our own perspective.

2. FLUORESCENT REPORTERS

The reporters frequently used in optical molecular imaging can be categorized into three major families: fluorescent proteins, organic fluorescent dyes, and inorganic fluorescent materials such as quantum dots. The common feature of these reporters is that they all absorb photons at certain wavelengths and reemit photons at slightly longer wavelengths. In order to probe a specific disease, monitor neurological activities, or track the distribution of a given drug, the reporters are usually transfected to cells, conjugated with ligands, antibodies, peptides, or tagged with targeting moieties. Depending on

Special Issue: Forum on Biomedical Applications of Colloidal Photoluminescent Quantum Dots

Received: November 26, 2012

Accepted: February 28, 2013

Published: February 28, 2013

applications, each family has its own advantages and drawbacks. They are briefly summarized below.

2.1. Fluorescent Proteins. The first isolated and purified fluorescent protein (FP) was green fluorescent protein (GFP). It is naturally found in *Aequorea victoria*, a species of jellyfish found in the waters of the northern Pacific Ocean. It has the property of absorbing blue light and then emitting green light, making it fluorescent. Up to date, GFP is still the most frequently used fluorescent protein as a biosensor.¹² However, the FPs currently being used by many researchers are the engineering modified forms of the original wild-type GFP. Changes were made to make them fluoresce at room temperature, to improve their quantum yields, to reduce their pH and chloride sensitivity, and to increase their photostability. In addition, researchers have modified GFP by directed and random mutagenesis to produce the wide variety of GFP derivatives.¹² The fluorescent emission range has been extended from the original green to either blue or red, covering nearly the entire visible spectrum. After the discovery of DsRed, the emission range has even been extended to the far-red spectral region. As we will see later, this is extremely important for *in vivo* fluorescence imaging, since only photons in the so-called “optical window”, with a wavelength of 650 to 900 nm, can penetrate a few centimeters in living tissue making *in vivo* whole body fluorescence imaging of small animal possible. However, the excitation maxima of available far-red FPs, including Katushka, are still located within the suboptimal wavelength range: 590 nm and lower. It remains one of the notable gaps for biochemists to develop a bright monomeric FP with an emission maximum peaking in the 650 to 900 nm spectral region for better and more efficient whole body small animal fluorescence imaging. FPs represent a unique basis of fluorescent reporters for visualizing and quantifying the enzymatic activity or conformational state of a protein of interest, changes in concentrations of particular molecules, and various physiological events *in vivo*, including living cells, tissues, or whole organisms.

The unique nature of FPs makes them quite different from the chemically synthesized sensitive fluorescent dyes, in terms of both development and application. One of the key differences is that FPs are delivered as genetic material by either transient transfections or transgenic techniques and are subsequently produced by cells themselves. Transgenic organisms expressing FPs can be created to monitor analyte concentrations, the activity of proteins of interest, and cell states *in vivo*, including tissues and cells that cannot be loaded with fluorescent dyes. In contrast to chemical dyes, FPs do not require external injection and are thus not prone to leakage during long-term experiments. The protein nature of FPs allows their targeting to virtually any cellular compartment or microcompartment through fusion with an appropriate signal domain.

Nowadays, FPs are very successful in visualizing various physiological events on the protein and cell levels. However, it still remains as a nontrivial challenge to precisely quantify the FP imaging results *in vivo*, because many parameters, such as brightness, can notably distort the results of quantitative *in vivo* experiments. Fluorescent brightness measured for an FP sample *in vitro* cannot be directly extrapolated to its actual brightness *in vivo*. Indeed, the signal brightness, generated by an FP expressed in living cells, is determined not only by its intrinsic spectral characteristics, but also by the cell expression level of the FP as well as the photostability and pH stability of the FP.

The cell expression level of an FP is affected by parameters such as the transcription and translation efficiency, the protein stability, and the chromophore maturation rate. The photostability of any given FP in a living cell depends on many parameters that are not yet well understood. The fluorescence of FPs typically increases at higher pH levels and reaches its maximum at a pH level between eight and nine. For most FPs developed to date, the fluorescence brightness depends on pH changes in the physiological range. Generally speaking, substantial pH changes are common in living environments during many physiological processes,¹³ resulting in considerable variations of FP-based *in vivo* imaging results. On the other hand, many FPs are prone to aggregation at high concentrations, which can be toxic for living cells, hindering work with cell cultures and thus making it impossible to generate stable cell lines and subsequently, healthy transgenic animals. Potential aggregation problems should always be kept in mind, especially with the expression of FPs in transgenic animals in order to balance the level of the fluorescence signal with the toxicity level of the FPs being used. For more details on many FPs, readers are encouraged to find out in the reviews^{14,15} by Chudakov et al.

2.2. Organic Fluorescent Dyes. Organic fluorescent dyes, or fluorophores, are the earliest and most common reporters used for *in vivo* fluorescence imaging. They are either free emissive molecules or conjugates of single fluorescent dyes to biological targeting moieties such as antibodies, antibody fragments, proteins, peptides, nucleic acids, or polysaccharides. Even unbound free emissive molecules can provide remarkable contrast of *in vivo* fluorescence imaging. Because of their small molecular size (within the range of a few kDa), they tend to circulate fast throughout the blood flow and bind to specific tissues by leaking through vessels. One example is indocyanine green (ICG). It exhibits strong albumin binding tendencies and shows a preferential uptake and retention in tumors. However, when bound to albumin, ICG's spectra are altered¹⁶ and its quantum yield decreases significantly (from approximately 15% in deionized water to 5% in blood).¹⁷

When conjugated to targeting moieties, organic fluorescent dyes can facilitate specific molecular bindings and the detection thereof. This is essential for the *in vivo* imaging of specific diseases, monitoring neurological activities, or tracking drug distribution in small animals. Organic dyes have been successfully bound to many antibodies and biological ligands for the *in vivo* imaging of tumors, atherosclerotic plaques, brain activities, as well as many other specific targets. In general, bioconjugates of organic fluorophores possess high target specificity; however, their *in vivo* imaging is often limited by a relatively low signal-to-background ratio, since unbound probes are also fluorescent and contribute to the background noise.^{18,19} Fortunately, with time domain technology, lifetime based *in vivo* fluorescence imaging can overcome this limitation by eliminating the contribution of unbound probes according to their distinct lifetimes, making it possible to interpret the *in vivo* imaging results with improved accuracy.

In recent years, a new group of organic fluorescent dyes, the so-called “activatable probes”,^{20–24} have been introduced, taking advantage of the fact that a molecule's fluorescence is intimately related to its physical and chemical environment. When two fluorochromes are within close proximity, fluorescence is significantly quenched. Two different types of activatable organic fluorophores, i.e. molecular beacons and enzyme-activatable probes, provide outstanding imaging signal-

to-background ratios upon binding to their molecular targets. Molecular beacons are single-stranded DNA fragments that have a fluorophore attached to one end and a quencher to the other.^{21,22} When the probe binds to a complementary strand of endogenous DNA or RNA within the cell, it unwinds and the fluorescent signal is generated. However, the fluorescent signal is typically weak. Furthermore, there is no effective method presently available for the *in vivo* intracellular delivery of the beacons so as to enable systemic molecular imaging in living animals. Enzyme-activatable probes usually consist of multiple organic fluorophores bound closely to one another on a backbone.^{23,24} The emissive agents are either conjugated directly or via a peptide spacer. Within the body, protease enzymes cleave either the construct backbone or the peptide spacer resulting in a strong increase in fluorescence signal-to-background ratio. These enzyme-sensing probes are useful for assessing activity in a number of diverse diseases, including mouse models of dysplastic intestinal adenomas, rheumatoid arthritis, and atherosclerosis.

Organic fluorescent reporters need to be administered to small animals for whole body *in vivo* fluorescence imaging. This may alter the physiological activities of small animals in many possible ways. Precise control of the actual amount of fluorophores injected to a small animal is one of the most important keys for quantitative fluorescence imaging. Proper characterization of the conjugation level of fluorophores with targeting moieties is another crucial aspect to ensure a reasonable and unbiased interpretation of the imaging results.

2.3. Quantum Dots. Fluorescent colloidal semiconductor nanocrystals, also known as quantum dots (QDs) or Qdots, another family of fluorescent reporters in optical molecular imaging, have attracted more and more attention in biological applications since 1998.^{25–28} Several characteristics distinguish Qdots from the reporters described above. Qdots typically are single crystals of a few nanometers in diameter, exhibiting size dependent absorption and emission. The absorption bands of Qdots are considerably wider than those of both fluorescent proteins and organic dyes, while the emission bands are narrow and more readily to be tuned from ultraviolet to the near-infrared (NIR) spectral range. This optical feature of Qdots does not only make it convenient to choose a practical excitation light source, but also renders it possible to completely eliminate excitation light leaking through fluorescent filters by setting the excitation wavelength far from the cutting edge of fluorescent filters, thus increasing the sensitivity of an imaging system. The broad absorption and narrow emission spectra of Qdots also make them perfect fluorescent reporters for spectrum multiplexed imaging as differently colored Qdots can be excited by the same wavelength of light. Another distinguishable characteristic of Qdots is their long fluorescence lifetime, which is typically a few nanoseconds to tens or over a hundred nanoseconds, much longer than that of proteins and organic dyes as well as tissue autofluorescence, which are usually less than a few nanoseconds. Thus, lifetime based background-free *in vivo* small animal imaging becomes practical when using Qdots together with time domain technology, as we will address later in this paper. It is also worth noting that the fluorescence lifetimes of Qdots can be modified through engineering by controlling their size. However, the dynamic optical properties of colloidal Qdots are a complicated issue and have not been well understood until now. Many parameters such as composition, size, and surface passivation affect the Qdots fluorescence lifetime.^{29–34}

Both single³¹ and multiple³³ exponential behaviors were reported for CdSe binary-based Qdots.

Toxicity is a main drawback of many Qdots because of the presence of heavy metals, such as Cd and Pb, in their cores, although different opinions were expressed.^{35–38} Surface modification (coating) could reduce toxicity, making Qdots suitable for various biomedical imaging applications. Detailed reviews of the Qdots' toxicity can be found in refs 36 and 37. Although numerous cytotoxic effects were observed with cell lines, little toxic effect was reported for small animals, like mice, at least for the dose used and during the experiment period.³⁷ In addition, a recent pilot study showed that there is no adverse response to intravenous injection of Qdots in nonhuman primates.³⁸

Surface modification can promote quantum yield of Qdots.³³ The other benefit of surface coating is to make Qdots water-soluble and thus have them interface with many biological entities. By choosing an appropriate coating ligand, a Qdot can be tagged to a specific antibody, a fragment of an antibody, a peptide, or an oligonucleotide, to form a single or combination of several recognition moieties targeting specific organs or diseased tissues for specific molecular imaging.^{39,40} Surface coating can also change Qdots into monitoring indicators for targeted drug delivery as well as disease therapy. Specifically surface coated Qdots have been used for various biomedical imaging applications, including imaging breast cancer and monitoring its treatment efficacy,⁴¹ imaging oral carcinoma,^{42,43} monitoring protease activity,⁴⁴ labeling murine bone marrow,⁴⁵ inhibiting cancer growth,⁴⁶ cancer targeting, and even imaging guided surgery.⁴⁷

3. TECHNOLOGIES FOR *IN VIVO* FLUORESCENCE IMAGING

3.1. Overview. There are a few approaches for *in vivo* small animal fluorescence imaging.⁶ In terms of the photon detector used, it can be either a charge-coupled-device (CCD) or a photomultiplier tube (PMT). The CCD usually has a larger field view resulting in a quick image acquisition. The PMT is usually more sensitive than a CCD. A system equipped with a PMT can have a variable field view by raster-scanning the imaging subject. The other important feature of a detector is its ability to record the temporal information of photons emitted from reporters, i.e. to acquire time-resolved data. This is crucial to properly interpreting the imaging results.

As for the excitation light source in an imaging system, it can be a broadband lamp or a laser. The laser itself can be continuous wave (CW) or pulsed. A broadband lamp usually covers a wide spectral range, suitable for many fluorescent reporters. However, a bandpass filter is required for a lamp to select a desired spectral band to excite a fluorescent reporter of interest. In practice, because of the imperfectness of the filter, a leakage of the excitation light to the fluorescent channel is unavoidable. This will contaminate the measured fluorescence signal and limit the specificity and the sensitivity of an imaging system. A laser is usually brighter than a lamp and has a narrow spectral band. A specific laser can be chosen to excite certain reporters. The narrow spectral band of the laser avoids the excitation light leaking to the fluorescent channel. Recently, wavelength tunable lasers have been used as the excitation light source in commercially available systems.^{48,49} In this kind of system, the laser wavelength can be tuned to match the excitation spectral band of fluorescent reporters to optimize the

excitation. A wavelength tunable laser combines the advantages of both the broadband lamp and the single wavelength laser.

Fluorescence is a transient phenomenon. If a pulsed excitation laser and a time-resolved detector are used, the temporal information of fluorescence photons can be recorded, allowing one to compute the fluorescent lifetimes of reporters. As we will see later, there are a few advantages to using fluorescent lifetime in small animal optical molecular imaging. The other benefit of time-resolved measurement is to use the time-of-flight information of the detected signal to precisely determine the origins of the fluorescence photons, i.e., location of the fluorescent reporters.

In terms of imaging configuration, depending on the placement of excitation light source and photon detector, an imaging system can be either a trans-illumination (source/detector in the opposite sides of a sample) or an epi-illumination (source/detector in the same side of a sample). The two configurations are also known respectively as transmission and reflection modes. The fluorescence signal in reflection mode is always less attenuated for fluorescent sources located in the first half of the sample due to an overall shorter photon path length. The transmission mode has an advantage if the fluorescent sources are located in the second half of the sample. However, if the sample is flipped over, again the reflection has a superior sensitivity compared to the transmission mode. On the other hand, the signal measured in transmission mode is relatively less dependent on the location of a fluorescent reporter if the imaging sample has a uniform thickness. However, it is not practical to expect uniform thickness and optical properties when imaging subjects in realistic *in vivo* imaging contexts, e.g., when imaging a mouse. As a result, it is quite challenging for an imaging system to simultaneously measure fluorescence signals from various regions along with a largely varied sample thickness. Compromise is always required in this case.

3.2. Challenges. In fluorescent microscopy, excitation photons directly illuminate a sample, and fluorescence photons directly reach the detector through a fluorescent filter. For *in vivo* small animal fluorescence imaging, the scenario is more complicated. Figure 1 is a schematic illustrating the scenario.

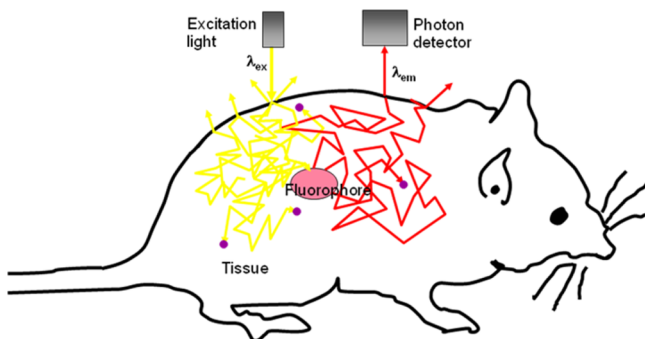


Figure 1. Schematic of photon propagation related to fluorescence process in tissue.

The excitation photons illuminate the skin of a small animal. Some of the photons will be reflected or scattered away, and some of the photons will go through the skin and propagate inside the animal tissue. The photon propagation in living tissue is completely different from the photon propagation in air. First, photons will suffer a certain number of scattering processes. The average free path length for NIR photons in

tissue is about 1 mm. In other words, their directions of propagation will be randomized after traveling through only 1 mm of tissue. Second, a big part of the photons will be absorbed by tissue chromophores during their propagation. Some of these chromophores will emit fluorescence photons. This is the so-called tissue autofluorescence (not shown in Figure 1). As a result, only a small portion of photons will reach the fluorescent reporter deep inside the animal. The reporter absorbs these excitation photons and emits fluorescence photons at a longer wavelength. The fluorescence photons will then propagate in tissue in a manner similar to the excitation photons. Only a small portion of these photons can reach the skin of the animal. Part of them will escape from the skin and some of them will reach the detector through a fluorescent filter.

The above scenario can help us identify the challenges of *in vivo* fluorescence imaging. First, the attenuation of light is severe due to photon scattering and absorption (together also known as diffusion). In the NIR spectral range, i.e., the so-called optical window, for every 2 mm of photons traveling, the attenuation is about 1 order of magnitude. In the visible spectral range, the attenuation is even more severe. This is why it is more efficient to use NIR light than visible light for whole body *in vivo* optical imaging of small animals. It also implies that the detector used in an *in vivo* imaging system must be very sensitive in order to detect a large enough number of photons coming from fluorescent reporters deep inside tissue.

Second, the requirement for fluorescent filter is higher. In fluorescent microscopy, the fluorescence signal is about one or 2 orders of magnitude smaller than the excitation light. For *in vivo* fluorescence imaging, the fluorescence signal in front of the filter is much smaller than the excitation light, depending on the location of the reporter inside the tissue.

Third, if the fluorescent emission band of a reporter overlaps with tissue autofluorescence, the signal detected will be contaminated. There is a wide variety of chromophores present in living tissue that can act as sources of autofluorescence.^{50,51} Examples include tryptophan, NADH, pyridoxine, collagen, elastin, flavins, porphyrins as well as the chlorophyll present in animal food. Most of them can be found in animal skin. As a result, tissue autofluorescence is often stronger than the fluorescence signal from a reporter deep inside tissue.

In addition, due to the photon diffusion in tissue, there is no straight link between a location on animal surface where a fluorescence photon is detected and the origin of the photon, i.e. the reporter's location. A model based correction must be applied to the measured signal in order to recover the reporter's location. From this point of view, no matter how high is the spatial resolution of a detector (e.g., a high-resolution CCD) used in an *in vivo* imaging system, the spatial resolution of mapping the result image to the location of a reporter of interest will be mainly determined by the level of diffusion and the accuracy of correction model employed.

3.3. Deep Tissue Fluorescence Lifetime Imaging Using a High Dynamic Range Raster-Scan System.

There are numerous systems commercially available for *in vivo* small animal fluorescence imaging. Each of them addresses the challenges aforementioned from different aspects. Detailed reviews of these systems can be found in ref 6. However, none of these systems provides *in vivo* fluorescence lifetime. In this paper, we will focus on an *in vivo* fluorescence lifetime imaging system, the Optix MX3, developed by ART Advanced Research Technologies Inc. (Montreal, Canada). Based on time domain

approach, the Optix MX3 system is configured in reflection geometry with a pulsed laser(s) as the excitation light source(s), a fluorescent filter(s) as the first-order hardware spectral unmixing component, and a PMT coupled with a time correlated single photon counting (TCSPC) board as the detection module. The system is fully automated and computer controlled. A special software package, OptiView, is dedicated to model-based data analysis. A schematic of the Optix MX3 system is shown in Figure 2 and some of its characteristics as well as the design rationales are described below.

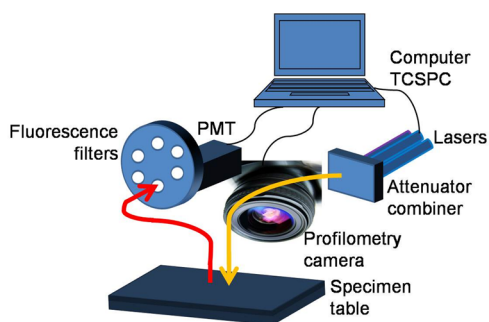


Figure 2. Schematic of the Optix MX3 time domain in vivo fluorescence imaging system.

a. Spectral Coverage. The Optix MX3 system incorporates 10 fluorescent filters, a combination of bandpass and long-pass with cut-offs and bandwidths optimized for maximizing the collection of any fluorescent emissions in the Vis-NIR spectral range (480 to 900 nm). The Optix MX3 system equipped with a wavelength tunable (480 to 785 nm) pulsed laser can excite any fluorescent reporter in the entire Vis-NIR spectral range. The filters and the laser(s) are integrated in the system with a flexible and fully computer controlled platform for the multispectral imaging of single or multifluorescent probe cocktails.

b. Rejection Ratio of Fluorescent Filters. The system is designed for performing raster-scans using point-illumination and point-detection configuration. The illumination and detection spots are separated at an optimized distance that suppresses background signal in fluorescence measurement. This approach provides an additional increase of the filter's rejection power for background noise by more than 2 orders of magnitude comparing to a typical full-field view illumination and a CCD detection. This feature makes Optix very sensitive for in vivo fluorescence imaging.^{52,53} It allows Optix to explore reporters deeper inside animal tissue and/or visualize lower concentration of reporters.

c. Sensitivity. The sensitivity of an imaging system refers to its ability to detect signal from very low amounts of fluorescent reporters of interest. Given the challenges of in vivo optical molecular imaging, sensitivity contains two folds of meaning: first, the system must be able to detect a very small number of fluorescence photons from the reporter of interest; second, the system must be able to separate these photons from those unwanted noise photons. Optix is specifically designed to address both aspects. PMT coupled with TCSPC is used in the detection channel to detect a very low level of optical signal. Background noise (tissue autofluorescence, excitation light leakage) is the main issue degrading the true sensitivity of an in vivo imaging system. The special design of point-illumination and point-detection configuration in Optix renders it to

maximize the physical rejection ability of fluorescent filters. Using fluorescence lifetime information, as we will see later, one can further increase the sensitivity and accuracy by differentiating the photons from reporter of interest and that from the background noise if it is not avoidable in the measured signal.

d. System Dynamic Range. Light attenuation has exponential function dependence over many factors, such as reporter location (depth) and tissue optical properties. For this reason, the signal counts of a reporter at two locations might be quite different (by orders of magnitude) even if the concentrations of the reporter at the two locations are very close. To properly detect them in a single image, a large dynamic range is required for the imaging system.

With a pixel-wise automatic adjustment of laser power and exposure time, Optix MX3 has a dynamic range of 9 orders of magnitude, or 90 dB, which is equivalent to a 30-bit CCD camera. This extended dynamic range allows users to simultaneously image samples with a very large range of concentration variation, or reporters in largely varied locations (depths) in tissue.

e. Spatial Resolution. The fluorescent reporters of interest for in vivo optical molecular imaging are usually deep inside tissue. Due to the diffusion of photons, as described in the previous section, "Challenges", the photons coming out from a small volume located inside the tissue will spread over a significantly larger area on the tissue surface resulting a blurred image. In such condition, no matter how good is the spatial resolution of the camera used, it will not be able to display the real probe distribution inside an animal. From this point of view, a high resolution CCD camera does not bring added value to the in vivo fluorescence imaging, except adding some cost. It seems that a raster-scan system using an optimized illumination-detection spot size performs better when imaging diffusing media, as demonstrated by De la Zerda et al., where Optix has better spatial resolution than a system equipped with a high-resolution CCD camera.⁵⁴

The XY resolution mentioned here is drawn from 2D images directly obtained by the imaging system before 3D tomographic reconstruction. By combining the time-of-flight information measured at different locations relative to the fluorescent source through 3D tomographic reconstruction,⁵⁵ the spatial resolution of Optix is significantly improved.

f. Limitation. As Optix is configured in raster-scan mode, every pixel in an image is mapped from the data acquired at a scanned point. The data contains rich information, but it perhaps takes longer time than a CCD based system to acquire large images. The typical scan time of Optix is a few minutes for a whole-body mouse image. This may limit its applications to some special cases, for example, to continuously track pharmacokinetic behaviors of some reporters in a time scale of a few seconds.

4. IN VIVO FLUORESCENCE LIFETIME IMAGING

Fluorescence lifetime is the average amount of time a fluorophore remains in its excited state following excitation. In time domain, measured fluorescence signal decreases exponentially over time. If the decrease follows a single exponential decay model, fluorescence lifetime can be obtained from the time at which the signal intensity decreases to 1/e (63%) of its initial value.⁹ On a logarithmic scale, the slope of a decay curve is the inverse of lifetime. In practice, lifetime is

obtained by fitting a set of measured data with some predefined models.

There are several advantages of using lifetime in fluorescence imaging. First, since lifetime is an intrinsic characteristic of a fluorescent reporter, it provides another specificity parameter to distinguish fluorescent reporters. Lifetime can be used to differentiate fluorescence photons from different reporters and/or tissue autofluorescence.⁵⁶ Lifetime can also be used to differentiate a reporter being in bound or unbound states.^{8,57} Second, for certain fluorescent reporters, their lifetime is sensitive to their micro biological environment, such as pH,^{13,58–60} Ca⁺, oxygen concentration,⁶¹ etc. In these cases, lifetime can be used to sense the micro environmental condition of neighboring tissues that are important for cancer research. In addition, lifetime is independent of signal amplitude that is a function of many factors such as reporter concentration, light attenuation, excitation laser power, etc. Therefore, lifetime is a more reliable “signature” and a convenient parameter for interpreting experiment results. FLIM technique is well accepted by the microscopy community and exhibits its advantages in numerous in vitro applications.⁶² Fluorescence lifetime estimation of in vivo data is more challenging since the effect of photon diffusion needs to be taken in account.^{63,64} Nevertheless, the advantages of FLIM also stand for in vivo fluorescence lifetime imaging. Below, we elaborate these advantages through a few application examples.

4.1. Differentiating Reporter in Bound or Unbound States. When a targeted fluorescent reporter is injected to an animal, some will bind with the target, and some will freely circulate in the blood flow. The fluorescence lifetimes of bound reporter and unbound reporter are different. The mechanism of what causes the lifetime difference is not well understood. One hypothesis is that when a reporter is bound to a target, its mobility is reduced, resulting in a longer lifetime of the reporter-target entity. The other hypothesis is that the energy of bound reporter acquired during excitation is transferred to the target through nonradiative channel instead of relaxing to ground state by emitting a fluorescence photon. The increased nonradiative energy transfer will also increase the lifetime of a fluorescent reporter. However, both hypotheses have not yet been directly proven by specifically designed experiment. Nevertheless, the observed lifetime difference can be used to differentiate a reporter in its bound from unbound states. Shown in Figure 3 is an example⁵⁷ of this application using the

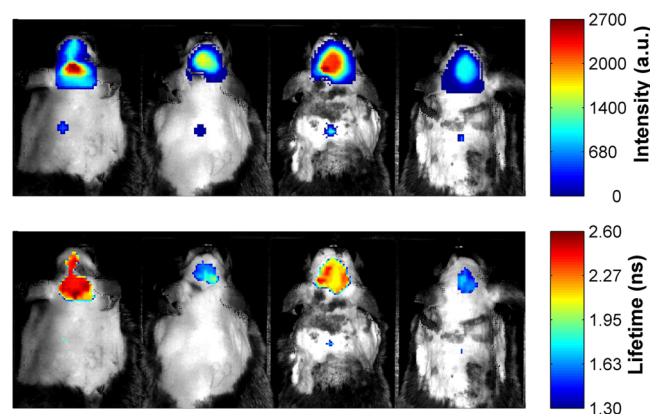


Figure 3. Fluorescence intensity (top) and lifetime (bottom) images acquired using an Optix imaging system for mice injected with AOI987. Refer to text for details.

Optix MX3 system. The images are four different mice, from left to right: an Alzheimer disease mouse with AOI987⁶⁵ probe bound to β amyloid plaques; an Alzheimer disease mouse without any probe; a wild type mouse with the AOI9087 present in the brain unbound; and a wild type negative control. The intensity images in the top panel show similar fluorescence signals from all the four mouse brains, while the lifetime images in the bottom panel help us to differentiate the source of these fluorescence signals. This can potentially be used as a parameter to diagnose Alzheimer disease and monitor its treatment if a therapy drug is administrated.

4.2. Sensing pH In vivo. As mentioned before, the lifetimes of certain fluorescent reporters are sensitive to their microenvironments, such as pH,^{13,58–60} Ca⁺, oxygen concentration,⁶¹ and so on. This makes it possible to use lifetime to detect possible alterations of physiological parameters (e.g., pH) resulting from malignant transformations of tissue, aiming for an earlier cancer detection. Below is an example⁵⁹ of sensing the local pH microenvironment by FLIM in vivo.

The fluorescent reporter used in the study is a pH sensitive organic dye, SNARF-1⁶⁶ (Invitrogen, Grand Island, NY). In this preliminary study, SNARF-1 mixed with matrigel at different biologically relevant pH levels were implanted in several mice. The mice were then imaged using the Optix system. Shown in Figure 4 are the result images. In location A,

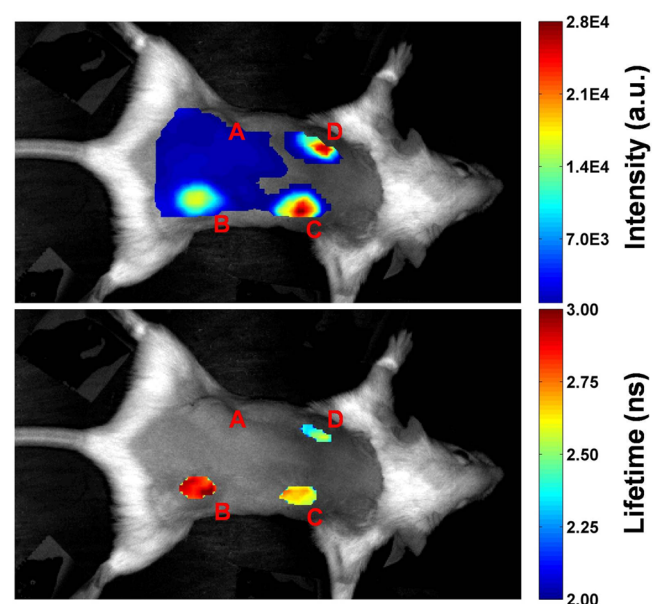


Figure 4. In vivo fluorescence intensity (top) and lifetime (bottom) images of a mouse implanted four samples with different pH values. The samples are clearly differentiated by FLIM attributed to pH.

the matrigel-only sample is implanted; B, C, and D are respectively the locations of SNARF-1 matrigel mixtures with pH 6, 7, and 8. The intensities (top image) from the pH samples are slightly different while the signal from the matrigel-only sample is comparable to that of the tissue autofluorescence. However, the fluorescence lifetimes from the three pH-varied samples are clearly different (bottom image and Table 1), ranging from 2.4 to 2.9 ns. These results demonstrate that FLIM can be used in vivo to sense the local pH microenvironment, which could find many applications in cancer research and other fields.

Table 1. Lifetime Values of the 4 pH Samples

sample	pH	lifetime (ns)
A	matrigel	NA
B	6	2.86
C	7	2.62
D	8	2.39

4.3. Lifetime unmixing. Fluorescence lifetime, fluorescence excitation, and emission spectra are unique and intrinsic characteristics of each fluorescent reporter. Sets of emission selective fluorescent filters are used in many imaging systems to perform spectral unmixing in order to distinguish different fluorescent reporters. However, if the fluorescent emission spectra of the reporters are overlapped, it is impossible to separate them by mere spectral unmixing. On the other hand, fluorescence lifetime is part of the time domain measurement results. If there is more than one component contained in the measured signal, one can unmix them through multilifetime analysis, even if the emission spectra are overlapped.^{67,68} In some other cases, one can directly separate signals from different fluorescent reporters by unmixing the measured temporal decay curve with known features of the components.⁶⁹ Similar to spectral unmixing, if the fluorescence lifetimes of reporters are very close, lifetime unmixing is not applicable.

Figures 5 and 6 are examples⁶⁷ of unmixing two fluorescent reporters based on dual lifetime analysis. In the experiment,

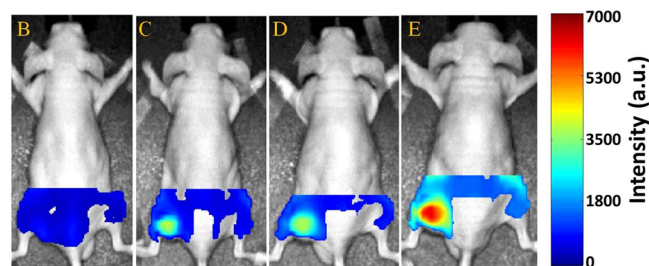


Figure 5. Fluorescence intensity images from mixture of DY682 labeled Transferrin and Cy5.5 labeled antibody 225, both targeting U87MG tumor cells implanted in the left flanks of mice. Images B, C, D, and E correspond to different fractions of Tf-DY682 and 225-Cy5.5.

mixtures of DY682 (Dyomics, Jena, Germany) labeled Transferrin (Tf-DY682) and Cy5.5 (GE Healthcare Bio-Sciences, Piscataway, NJ) labeled antibody 225 (225-Cy5.5) at varied fraction ratios were injected in mice bearing U87MG (a human primary glioblastoma cell line) tumor in their left flanks. The Tf and the antibody 225 are both targeting the U87MG tumor. DY682 and Cy5.5 have overlapped excitation and emission spectra. Using the same excitation laser, the emission signals are detected in the same measurement. In Figure 5, we see the intensity images of the mixed signals measured using the same fluorescent filter. With dual lifetime analysis, one can unmix the contributions from the two components in the measured fluorescence signals. In Figure 6, the unmixing results are shown. The top panels display the percentage contributions of 225-Cy5.5, and the bottom panels correspond to the percentage contributions of Tf-DY682. The recovered fractions are consistent with the fractions in the mixtures.

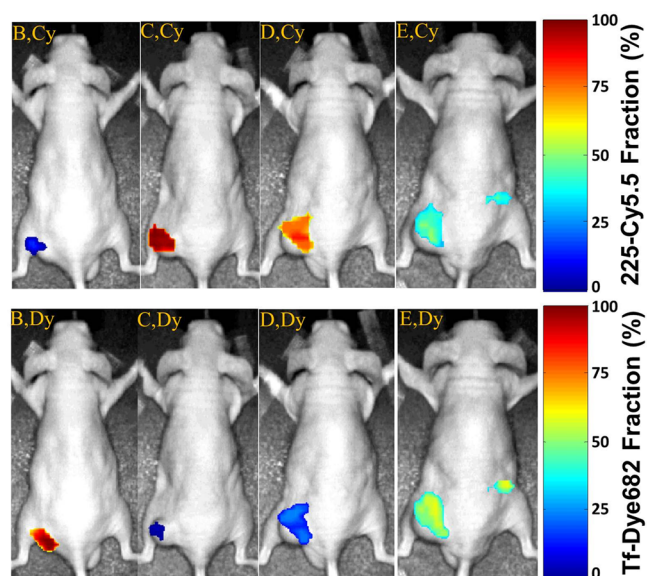


Figure 6. Relative fractions in percentage of 225-Cy5.5 (top panels) and Tf-DY682 (bottom panels). The 225-Cy5.5 fraction of image C is $\sim 100\%$ and the Tf-682 fraction is ~ 0 , because this panel is injected with only 225-Cy5.5. Similarly, the Tf-Dy682 fraction of panel B is $\sim 100\%$, whereas the 225-Cy5.5 fraction is very small.

4.4. Background-Free In vivo Imaging Using Quantum Dots. As aforementioned, Qdots have some unique characteristics for in vivo fluorescence imaging. One of that is their long fluorescence lifetime. It is much longer than that of any fluorescent proteins and organic dyes including the tissue autofluorescence. This fact makes it possible to conduct background-free in vivo imaging using Qdots. The principle is simple. When a mouse bearing Qdots is imaged, the fluorescence signal from Qdots together with any other signals, including the tissue autofluorescence and possibly the leaking of the excitation photons with wavelength falling in the passing band of the fluorescent filter, will be recorded by the imaging detector and presented in the result image. Fortunately, the photons from Qdots and other sources have some different intrinsic characteristics, such as fluorescence lifetime. Therefore, one can separate the Qdots signal from others according to their fluorescence lifetimes. Shown in Figure 7 is an example demonstrating this principle.

In the experiment, 20 μL of Qdot 705 at concentrations of 62 and 125 nM were subcutaneously injected to a CD1 mouse respectively on its right and left back position. Qdot 705 was favorably chosen as the fluorescent reporter due to its NIR fluorescent emission with peak at 705 nm, more efficient for in vivo imaging. Detail information of Qdot 705, such as size, material structure, and spectral characteristics can be found elsewhere.⁶⁶ After injection, the mouse was scanned on the Optix imaging system with regions of interest covering the two injection spots as well as some other parts of the mouse body. The excitation light was a 670 nm pulsed diode laser operated at 2.5 MHz repetition frequency. A long-pass filter with cutoff at 695 nm was used for fluorescence detection.

The acquired fluorescence intensity image is shown in the top panel of Figure 7. The signals from the two injection spots are strong, but the signals from other parts are not zero although they are not as strong as that from the injection spots. The fluorescence lifetime image is shown in the middle panel of Figure 7. One may notice that the fluorescence lifetimes near

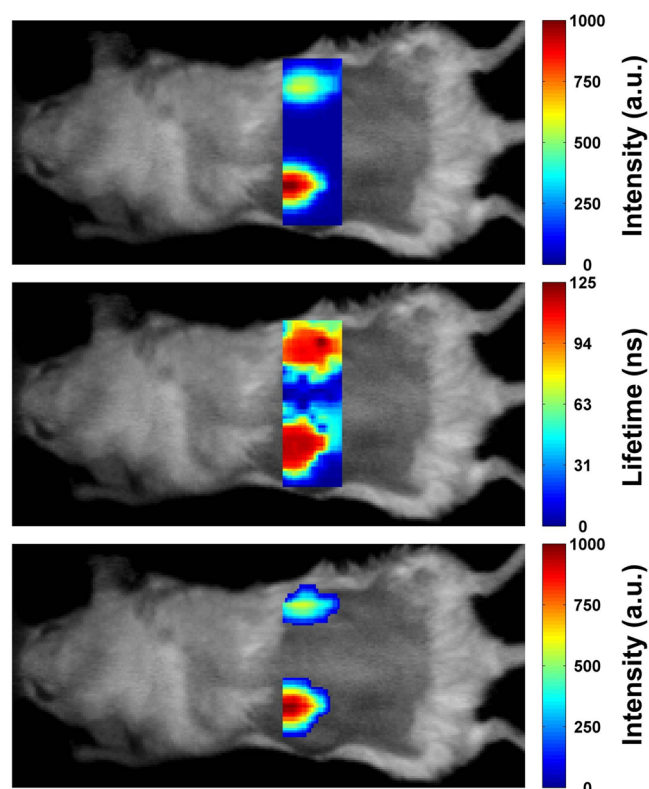


Figure 7. Fluorescence intensity (top and bottom panel) and lifetime (middle panel) images of Qdot 705 subcutaneously injected in a mouse. Fluorescence lifetime helps to differentiate signals from Qdot 705 and other sources. Background-free fluorescence image of Qdot 705 (bottom panel) is obtained after applying lifetime gating (>90 ns) to the intensity image directly acquired (top panel) by an Optix imaging system.

the two injection spots are similar (about 100 ns) despite the concentration of Qdot 705 on the left side being doubled, proving that lifetime is independent of concentration. The lifetime in regions far from the injection spots corresponds mainly to tissue autofluorescence. In regions surrounding the injection spots, the lifetime values are shorter than that of Qdot 705 but much longer than that of tissue autofluorescence, since the fluorescence signals from these regions consist of contributions from both diffused Qdot 705 fluorescence and tissue autofluorescence. The resulted lifetime is the weighted combination of the two. When using fluorescence lifetime of Qdot 705 as a threshold, one can “clean” the fluorescence intensity image shown in the top panel of Figure 7. The process is also called lifetime gating. Based on lifetime image, as shown in middle panel of Figure 7, one can build a gating mask. For every pixel in the image, if its lifetime value τ is close to that of Qdot 705 (here we use $90 \text{ ns} < \tau < 110 \text{ ns}$), a value of 1 is assigned. For all pixels with lifetime other than that of Qdot 705, a value of 0 is assigned. Mathematically, the gating mask is

$$g_{ij} = \begin{cases} 1 & \text{if } 90 \text{ ns} \leq \tau_{ij} \leq 110 \text{ ns} \\ 0 & \text{if } \tau_{ij} < 90 \text{ ns} \text{ or } \tau_{ij} > 110 \text{ ns} \end{cases}$$

When this 1/0 gating mask is multiplied with the intensity image I_{ij}^{raw} , as shown in the top panel of Figure 7, a new image I_{ij}^{clean} (bottom panel of Figure 7) is generated. In this new image, only pixels satisfying the lifetime gating criterion of

Qdot 705 show up and all other pixels associated with tissue autofluorescence are eliminated, therefore a background-free intensity image is obtained.

It is worth to note that in the example the Qdot 705 is injected subcutaneously so that light attenuation due to diffusion is not severe in this case. As a result, the signal from Qdot 705 is much brighter than that from other sources, e.g. tissue autofluorescence. However, when Qdots are located deep inside the mouse, like the cases encountered in most practical experiments, light attenuation will be much severe. Therefore the Qdots signal will be much weaker compared to the tissue autofluorescence (mainly generated from the skin of mouse). There will be no “bright” spot to identify the Qdots in fluorescence intensity view. In those cases, it will be particularly important to use lifetime gating in order to achieve background-free in vivo Qdots fluorescence imaging.

In addition to lifetime gating technique, there is another way to achieve background-free in vivo fluorescence imaging using Qdots when using time domain technology. The long fluorescence lifetime of Qdots implies that the fluorescence decay of Qdots is slower and lasts longer. A time gate of the photon detector, either CCD or PMT, of an imaging system could be adjusted to open after the tissue autofluorescence and other organic dyes finish their decay, so the detector will record only the fluorescence photons from Qdots that will result in background-free fluorescence images directly by hardware. The drawback of this approach is that the photons corresponding to the decay peak of Qdots will be missed.

5. SUMMARY AND PERSPECTIVES

Compared to other imaging approaches, in vivo fluorescence optical molecular imaging is still in its development stage, although tremendous progresses have been made within the past decade. We have briefly reviewed the fluorescent reporters being used for in vivo fluorescence imaging, such as fluorescent proteins, organic fluorescent dyes, as well as quantum dots. Each has its own advantages and drawbacks. Various fluorescent reporters can be chosen depending on different applications. Tagging reporters to specific targeting moiety is essential to explore the true potential of in vivo fluorescence imaging in research for understanding the pathology of various diseases as well as developing new drugs to cure diseases, such as cancers, atherosclerosis, Alzheimer, and many others.

We have also briefly reviewed the technologies to detect fluorescence photons coming out from living small animals and to generate in vivo images, as well as the associated challenges. In early days, researchers were keen on fluorescent pictures taken on live animals injected with selected dyes or animals bearing fluorescent proteins through gene modification. The emission wavelengths are mostly in the visible spectral region. As we accumulate more and more knowledge related to in vivo fluorescence imaging, the emission wavelength of fluorescent reporter being used has shifted to NIR spectral region in order to probe locations deep inside living small animals. As to increasing the content of imaging results, it is not enough to only have in vivo fluorescent pictures. More demand has emerged, such as quantification, or differentiating measured fluorescence signals generated by targeted reporters from that by free reporters, to help better and more accurately interpret the imaging results. To fulfill such requirements, advanced imaging systems that can offer high content results, such as Optix, are required.

Fluorescence lifetime imaging is already well accepted by the community of microscopy imaging. Its advantages also hold for in vivo optical molecular imaging. We presented a few examples using fluorescence lifetime for advanced in vivo fluorescence imaging. Using lifetime, one can differentiate fluorescence signals generated by a reporter either bound to its target or in its free state. With certain pH-sensitive fluorescent reporters, one can also sense the pH state of the microenvironment using lifetime. For improving specificity, one can also label a target with two reporters and unmix the measured fluorescence signals based on fluorescence lifetimes.

Qdots, even if they are a relatively new family of fluorescent reporters, are very promising because of their spectral flexibility and long lifetimes. Their unique characteristic of long fluorescence lifetimes makes them easily distinguishable from any other reporters, including the unavoidable tissue autofluorescence in practical in vivo fluorescence imaging. Taking advantage of fluorescence lifetime provided by a time-domain imaging system, we demonstrated that background-free in vivo fluorescence imaging can be achieved using Qdots. It is a prelude for numerous in vivo applications. We expect readers to explore its full potential in every aspect to advance the imaging technology using Qdots.

AUTHOR INFORMATION

Corresponding Author

*E-mail: gbma98@gmail.com.

Notes

The author declares no competing financial interest.

ACKNOWLEDGMENTS

The author thanks Dr. K. Yu, Dr. A. Abedelnasser, Dr. N. Mincu, and Ms. M. Jean-Jacques for stimulating and fruitful discussions in preparing this manuscript.

ABBREVIATIONS

- CCD, charge-coupled-device
- CW, continues wave
- FLIM, fluorescence lifetime imaging
- FP, fluorescent protein
- GFP, green fluorescent protein
- ICG, indocyanine green
- NIR, near-infrared
- PMT, photomultiplier tube
- Qdots, quantum dots
- TD, time domain

REFERENCES

- (1) Chatziioannou, A. F. *Mol. Imaging Biol.* **2002**, *4*, 47–63.
- (2) Weissleder, R.; Ntziachristos, V. *Nat. Med.* **2003**, *9*, 123–128.
- (3) Herschman, H. R. *Science* **2003**, *302*, 605–608.
- (4) Meikle, S. R.; Kench, P.; Kassiou, M.; Banati, R. B. *Phys. Med. Biol.* **2005**, *50*, R45–61.
- (5) Kepshire, D.; Mincu, N.; Hutchins, M.; Gruber, J.; Dehghani, H.; Hypnarowski, J.; Leblond, F.; Khayat, M.; Pogue, B. W. *Rev. Sci. Instrum.* **2009**, *80*, 043701.
- (6) Leblond, F.; Davis, S. C.; Valdes, P. A.; Pogue, B. W. *J. Photochem. Photobiol. B* **2010**, *98*, 77–94.
- (7) Berezin, M. Y.; Achilefu, S. *Chem. Rev.* **2010**, *110*, 2641–2684.
- (8) Ardeshirpour, Y.; Chernomordik, V.; Zielinski, R.; Capala, J.; Griffiths, G.; Vasalatiy, O.; Smirnov, A. V.; Knutson, J. R.; Lyakhov, I.; Achilefu, S.; Gandjbakhche, A.; Hassan, M. *PLoS One* **2012**, *7*, e31881.
- (9) Lakowicz, J. R. *Principle of Fluorescence Spectroscopy*, 2nd ed.; Kluwer Academic/Plenum Publishers: New York, 1999.
- (10) Contag, P. R.; Olomu, I. N.; Stevenson, D. K.; Contag, C. H. *Nat. Med.* **1998**, *4*, 245–247.
- (11) Robertson, R.; Germanos, M. S.; Li, C.; Mitchell, G. S.; Cherry, S. R.; Silva, M. D. *Phys. Med. Biol.* **2009**, *54*, N355–365.
- (12) Shaner, N. C.; Steinbach, P. A.; Tsien, R. Y. *Nat. Methods* **2005**, *2*, 905–909.
- (13) Srivastava, J.; Barber, D. L.; Jacobson, M. P. *Physiology* **2007**, *22*, 30–39.
- (14) Chudakov, D. M.; Lukyanov, S.; Lukyanov, K. A. *Trends Biotechnol.* **2005**, *23*, 605–613.
- (15) Chudakov, D. M.; Matz, M. V.; Lukyanov, S.; Lukyanov, K. A. *Physiol. Rev.* **2010**, *90*, 1103–1163.
- (16) Landsman, M. L.; Kwant, G.; Mook, G. A.; Zijlstra, W. G. *J. Appl. Physiol.* **1976**, *40*, S75–S83.
- (17) Licha, K.; Riefke, B.; Ntziachristos, V.; Becker, A.; Chance, B.; Semmler, W. *Photochem. Photobiol.* **2000**, *72*, 392–398.
- (18) Licha, K.; Olbrich, C. *Adv. Drug Delivery Rev.* **2005**, *57*, 1087–1108.
- (19) Bremer, C.; Ntziachristos, V.; Weissleder, R. *Eur. Radiol.* **2003**, *13*, 231–243.
- (20) Goergen, C. J.; Chen, H. H.; Bogdanov, A.; Sosnovik, D. E.; Kumar, A. T. *J. Biomed. Opt.* **2012**, *17*, 056001.
- (21) Tyagi, S.; Kramer, F. R. *Nat. Biotechnol.* **1996**, *14*, 303–308.
- (22) Achilefu, S. *Technol. Cancer Res. Treat.* **2004**, *3*, 393–409.
- (23) Tung, C. H.; Bredow, S.; Mahmood, U.; Weissleder, R. *Bioconjugate Chem.* **1999**, *10*, 892–896.
- (24) Weissleder, R.; Tung, C. H.; Mahmood, U.; Bogdanov, A., Jr. *Nat. Biotechnol.* **1999**, *17*, 375–378.
- (25) Bruchez, M.; Moronne, M.; Gin, P.; Weiss, S.; Alivisatos, A. P. *Science* **1998**, *281*, 2013–2016.
- (26) Chan, W. C. W.; Nie, S. *Science* **1998**, *281*, 2016–2018.
- (27) Michalet, X.; Pinaud, F. F.; Bentolila, L. A.; Tsay, J. M.; Doose, S.; Li, J. J.; Sundaresan, G.; Wu, A. M.; Gambhir, S. S.; Weiss, S. *Science* **2005**, *307*, 538–544.
- (28) Michalet, X.; Colyer, R. A.; Antelman, J.; Siegmund, O. H.; Tremisin, A.; Vallerga, J. V.; Weiss, S. *Curr. Pharm. Biotechnol.* **2009**, *10*, 543–558.
- (29) Nirmal, M.; Murray, C. B.; Bawendi, M. G. *Phys. Rev. B: Condens. Matter* **1994**, *50*, 2293–2300.
- (30) Nirmal, M.; Norris, D. J.; Kuno, M.; Bawendi, M. G.; Efros, A. L. *Phys. Rev. Lett.* **1995**, *75*, 3728–3731.
- (31) Fisher, B. R.; Eisler, H.-J.; Stott, N. E.; Bawendi, M. G. *J. Phys. Chem. B* **2004**, *108*, 143–148.
- (32) Van Driel, A. F.; Allan, G.; Delerue, C.; Lodahl, P.; Vos, W. L.; Vanmaekelbergh, D. *Phys. Rev. Lett.* **2005**, *95*, 236804.
- (33) Jakubek, Z. J.; Jonathan, de V.; Lin, S.; Ripmeester, J.; Yu, K. J. *Phys. Chem. C* **2008**, *112*, 8153–8158.
- (34) Ko, S. H.; Du, K.; Liddle, J. A. *Angew. Chem., Int. Ed.* **2013**, *52*, 1193–1197.
- (35) Kloepfer, J. A.; Mielke, R. E.; Wong, M. S.; Nealon, K. H.; Stucky, G.; Nadeau, J. L. *Appl. Environ. Microbiol.* **2003**, *69*, 4205–4213.
- (36) Tsay, J. M.; Michalet, X. *Chem. Biol.* **2005**, *12*, 1159–1161.
- (37) Pelley, J. L.; Daar, A. S.; Saner, M. A. *Toxicol. Sci.* **2009**, *112*, 276–296.
- (38) Ye, L.; Yong, K.-T.; Liu, L.; Roy, I.; Hu, R.; Zhu, J.; Cai, H.; Law, W.-C.; Liu, J.; Wang, K.; Liu, J.; Liu, Y.; Hu, Y.; Zhang, X.; Swihart, M. T.; Prasad, P. N. *Nat. Nanotechnol.* **2012**, *7*, 453–458.
- (39) Wu, C.; Hansen, S. J.; Hou, Q.; Yu, J.; Zeigler, M.; Jin, Y.; Burnham, D. R.; McNeill, J. D.; Olson, J. M.; Chiu, D. T. *Angew. Chem., Int. Ed.* **2011**, *50*, 3430–3434.
- (40) Mukthavaram, R.; Wrasidlo, W.; Hall, D.; Kesari, S.; Makale, M. *Bioconjugate Chem.* **2011**, *22*, 1638–1644.
- (41) Jung, K. H.; Choe, Y. S.; Paik, J. Y.; Lee, K. H. *J. Nucl. Med.* **2011**, *52*, 1457–1464.
- (42) Yang, K.; Zhang, F. J.; Tang, H.; Zhao, C.; Cao, Y. A.; Lv, X. Q.; Chen, D.; Li, Y. D. *Int. J. Nanomed.* **2011**, *6*, 1739–1745.
- (43) Yang, K.; Cao, Y. A.; Shi, C.; Li, Z. G.; Zhang, F. J.; Yang, J.; Zhao, C. *Oral Oncol.* **2010**, *46*, 864–868.

- (44) Biswas, P.; Cella, L. N.; Kang, S. H.; Mulchandani, A.; Yates, M. V.; Chen, W. *Chem. Commun.* **2011**, *47*, 5259–61.
- (45) Muccioli, M.; Pate, M.; Omozebi, O.; Benencia, F. J. *Vis. Exp* **2011**, DOI: 10.3791/2785.
- (46) Xu, W.; Liu, L.; Brown, N. J.; Christian, S.; Hornby, D. *Molecules* **2012**, *17*, 796–808.
- (47) Li, Y.; Li, Z.; Wang, X.; Liu, F.; Cheng, Y.; Zhang, B.; Shi, D. *Theranostics* **2012**, *2*, 769–76.
- (48) Mincu, N.; Huang, D.; Piche, M.; Ma, G. In *Proceedings of SPIE Photonics West: Reporters, Markers, Dyes, Nanoparticles, and Molecular Probes for Biomedical Applications III*; San Francisco, CA, Jan 22–27, 2011; Achilefu, S. and Raghavachari, R., Eds.; SPIE: Bellingham, WA, 2011; Vol. 7910, 79101K.
- (49) Mincu, N.; Marcil, F.; Thornhill, L.; Varvaris, S.; Roy, A.; Fortin, F.; Piché, M.; Ma, G. *World Molecular Imaging Congress*; San Diego, CA, Sept 7–10, 2011; World Molecular Imaging Society: Los Angeles, CA, 2011.
- (50) Richards-Kortum, R.; Sevick-Muraca, E. *Annu. Rev. Phys. Chem.* **1996**, *47*, 555–606.
- (51) Billinton, N.; Knight, A. W. *Anal. Biochem.* **2001**, *291*, 175–197.
- (52) Ma, G.; Gallant, P.; McIntosh, L. *Appl. Opt.* **2007**, *46*, 1650–1657.
- (53) Keren, S.; Gheysens, O.; Levin, C. S.; Gambhir, S. S. *IEEE Trans. Med. Imaging* **2008**, *27*, 58–63.
- (54) De la Zerda, A.; Bodapati, S.; Teed, R.; Schipper, M. L.; Keren, S.; Smith, B. R.; Ng, J. S.; Gambhir, S. S. *Mol. Imaging Biol.* **2010**, *12*, 500–508.
- (55) Lam, S.; Lesage, F.; Intes, X. *Opt. Express* **2005**, *13*, 2263–2275.
- (56) Ma, G.; Que, I.; Chan, A.; Lowik, C. *World Molecular Imaging Congress*; Dublin, Ireland, Sept 5–8, 2012; World Molecular Imaging Society: Los Angeles, CA, 2012.
- (57) Nabuurs, R.; Que, I.; Chan, A.; Ma, G.; Lowik, C.; Louise van der Weerd, L. *World Molecular Imaging Congress*; Kyoto, Japan, Sept 8–11, 2010; World Molecular Imaging Society: Los Angeles, CA, 2010.
- (58) Almutairi, A.; Guillaudeu, S. J.; Berezin, M. Y.; Achilefu, S.; Frechet, J. M. J. *Am. Chem. Soc.* **2008**, *130*, 444–5.
- (59) Ma, G.; Huang, D.; Mincu, N.; Jean-Jacques, M.; Khayat, M. *World Molecular Imaging Congress*; Kyoto, Japan, Sep 8–11, 2010; World Molecular Imaging Society: Los Angeles, CA, 2012.
- (60) Tang, R.; Lee, H.; Achilefu, S. *J. Am. Chem. Soc.* **2012**, *134*, 4545–4548.
- (61) Hosny, N. A.; Lee, D. A.; Knight, M. M. *J. Biomed. Opt.* **2012**, *17*, 016007.
- (62) Becker, W. J. *Microsc.* **2012**, *247*, 119–136.
- (63) Vishwanath, K.; Pogue, B.; Mycek, M. A. *Phys. Med. Biol.* **2002**, *47* (18), 3387–405.
- (64) Ma, G.; Fortier, S.; Jean-Jacques, M.; Mincu, N.; Leblond, F.; Ichalalene, Z.; Benyamin-Seeyar, A.; Khayat, M. In *Proceedings of SPIE Photonics West: Multimodal Biomedical Imaging III*; San Jose, CA, Jan 19–24, 2008; Azar, F. S.; Intes, X., Eds.; SPIE: Bellingham, WA, 2008; Vol. 6850, p 685003.
- (65) Hintersteiner, M.; Enz, A.; Frey, P.; Jatton, A.-L.; Kinzy, W.; Kneuer, R.; Neumann, U.; Rudin, M.; Staufenbiel, M.; Stoeckli, M.; Wiederhold, K.-H.; Gremlich, H.-U. *Nat. Biotechnol.* **2005**, *23*, 577–583.
- (66) Johnson I.; Spence M. T. Z. *Molecular Probes Handbook, A Guide to Fluorescent Probes and Labeling Technologies*, 11th ed; Invitrogen: Carlsbad, CA, 2010; www.invitrogen.com.
- (67) Ma, G.; Melanson-Drapeau, L.; Fortier, S.; Iqbal, U.; Mincu, N.; Stanimirovic, D.; Khayat, M.; Abulrob, A. *World Molecular Imaging Congress*; Nice, France, Sept 10–13, 2008; World Molecular Imaging Society: Los Angeles, CA, 2008.
- (68) Hall, D. J.; Han, S. H.; Chepetan, A.; Inui, E. G.; Rogers, M.; Dugan, L. L. *J. Cereb. Blood Flow Metab.* **2012**, *32*, 23–32.
- (69) Ma, G.; Guerrero, B.; Benyamin-Seeyar, A.; Khayat, M. OSA *Biomedical Optics Topical Meetings*; Fort St. Petersburg, FL, Mar 16–20, 2008; Optical Society of America: Washington, D.C., 2008.